Spin-1/2 Ising-Heisenberg model with the pair *XYZ* Heisenberg interaction and quartic Ising interactions as the exactly soluble zero-field eight-vertex model

Jozef Strečka,[1,*] Lucia Čanová,[2] and Kazuhiko Minami[3]
[1]*Department of Theoretical Physics and Astrophysics, Faculty of Science, P. J. Šafárik University, Park Angelinum 9, 040 01 Košice, Slovak Republic*
[2]*Department of Applied Mathematics, Faculty of Mechanical Engineering, Technical University, Letná 9, 042 00 Košice, Slovak Republic*
[3]*Graduate School of Mathematics, Nagoya University, Nagoya 464-8602, Japan*
(Received 3 February 2009; published 6 May 2009)

The spin-1/2 Ising-Heisenberg model with the pair *XYZ* Heisenberg interaction and quartic Ising interactions is exactly solved by establishing a precise mapping relationship with the corresponding zero-field (symmetric) eight-vertex model. It is shown that the Ising-Heisenberg model with the ferromagnetic Heisenberg interaction exhibits a striking critical behavior, which manifests itself through re-entrant phase transitions as well as continuously varying critical exponents. The changes in critical exponents are in accordance with the weak universality hypothesis in spite of a peculiar singular behavior that emerges at a quantum critical point of the infinite order, which occurs at the isotropic limit of the Heisenberg interaction. On the other hand, the Ising-Heisenberg model with the antiferromagnetic Heisenberg interaction surprisingly exhibits less significant changes in both critical temperatures and critical exponents upon varying the strength of the exchange anisotropy in the Heisenberg interaction.

DOI: 10.1103/PhysRevE.79.051103 PACS number(s): 05.50.+q, 75.10.Jm

I. INTRODUCTION

Over the last six decades, exactly solvable models of interacting many-body systems have attracted considerable attention due to their uncoverable role in a fundamental understanding of order-disorder phenomena [1–3]. In particular, exactly solvable quantum spin models are currently at the forefront of theoretical research interest as they often exhibit a peculiar interplay between quantum fluctuations and cooperativity [4–6]. Despite extensive studies, however, phase transitions and critical phenomena of rigorously solved quantum spin models still belong to the most challenging unresolved issues to deal with, since quantum fluctuations usually prefer the lack of spontaneous order. Indeed, there are only few exactly solved quantum spin models that simultaneously exhibit both spontaneous long-range order and obvious quantum manifestations.

It has been recently demonstrated that the spontaneous order, which is accompanied with obvious quantum manifestations, might be an inherent feature of the hybrid Ising-Heisenberg planar models [7] whose lattice sites are in part occupied by the Ising spins and partly by the Heisenberg spins [8–17]. Note that all aforementioned Ising-Heisenberg planar models have exactly been solved with the help of suitable algebraic transformations such as the decoration-iteration [18] or the star-triangle [19] transformation, which establish a precise mapping equivalence with the corresponding spin-1/2 Ising model. It is worthwhile to recall, moreover, that the decoration-iteration and star-triangle mapping transformations were substantially generalized by Fisher [20] (see also for details Ref. [21]), who first pointed out that in principle arbitrary quantum-mechanical system coupled to two or three outer Ising spins can be replaced via appropriate algebraic transformation by the equivalent expression containing pairwise spin-spin interactions between the outer Ising spins. In such a way, one effectively establishes a precise mapping relationship that connects the exact solution of some original model (which might describe a rather complex quantum-mechanical system) with the exact solution of the corresponding spin-1/2 Ising model, which is generally known for many planar lattices of different topologies [1,3,21–24].

On the contrary, there does not exist a general algebraic transformation for any quantum-mechanical system coupled to four or more outer Ising spins if one considers pairwise interactions between the outer Ising spins only [20]. Rojas *et al.* [25] recently found exact evidence that it is nevertheless possible to include multispin interactions between the outer Ising spins into the algebraic transformation in order to ensure its general validity. Thus, the algebraic transformation with effective pair and quartic interactions is, for instance, required when searching for an exact treatment of the quantum-mechanical system coupled to four outer Ising spins in the absence of the external field. The spin-1/2 Ising model with pair and quartic interactions is however nothing but the alternative definition of the general eight-vertex model [26,27], which becomes exactly tractable by imposing a special additional constraint to its vertex energies (Boltzmann's weights) known either as Baxter's zero-field (symmetric) condition [1,28,29] or the free-fermion condition of Fan and Wu [30,31]. Bearing all this in mind, one could intuitively expect that there might exist a certain class of exactly solvable quantum-mechanical spin models for which the appropriate algebraic transformation yields a precise mapping correspondence to the eight-vertex model generally satisfying Baxter's zero-field condition [1,28,29]. The main goal of the present work is to show that the spin-1/2 Ising-Heisenberg model with the pair *XYZ* Heisenberg interaction and the quartic Ising interactions falls into this class of fully exactly soluble models.

*jozef.strecka@upjs.sk, jozkos@pobox.sk

The importance of exact results to be obtained for the Ising-Heisenberg model with the pair and quartic interactions should be viewed in more respects. First, it is well known that the quartic interaction basically affects magnetic properties of several insulating copper compounds such as La_2CuO_4 [32–37] (undoped parent compound for high-T_c cuprates), $SrCu_2O_3$ [35], $La_6Ca_8Cu_{24}O_{41}$ [38], and $La_4Sr_{10}Cu_{24}O_{41}$ [39]. Even though it would be rather striking coincidence if some real magnetic material would obey very specific topological requirements of the model under investigation, it is quite reasonable to suspect that our exact results might at least shed light on some important aspects of the critical behavior of real magnetic materials. Second, our model system represents a rare example of the exactly solved lattice-statistical model, which contradicts the standard universality hypothesis in that its critical exponents vary continuously with the interaction parameters over the full range of possible values of the critical exponents. Third, the exactly soluble vertex models have found over the last few decades manifold applications in seemingly diverse research areas. Exact solutions of vertexlike models essentially tackle the problem of the residual entropy of two-dimensional ice [40,41], the Slater model of hydrogen-bonded ferroelectrics [42–44], the integrable quantum spin models such as the quantum Heisenberg chain [43,45–50], the ice-type solid-on-solid (SOS) model [48,49,51,52], the problem of counting domino tilings [31,53–56], the three- and four-coloring problems of the square and hexagonal lattices [1,41,57–59], etc.

The rest of this paper is organized as follows. In Sec. II, we will provide the detailed description of the hybrid Ising-Heisenberg model, and then, basic ideas of the exact mapping to the zero-field eight-vertex model will be explained. This is followed by the presentation of the most interesting results for the ground-state and finite-temperature phase diagrams, which are supplemented by a detailed analysis of a rather strange nonuniversal behavior of critical exponents. Finally, some concluding remarks are given in Sec. IV.

II. ISING-HEISENBERG MODEL AND ITS EQUIVALENCE TO THE ZERO-FIELD EIGHT-VERTEX MODEL

Consider a two-dimensional lattice of edge-sharing octahedrons, each of them with four Ising spins $\sigma=1/2$ in a basal plane and two Heisenberg spins $S=1/2$ in apical positions, as schematically depicted in Fig. 1. Suppose furthermore that each edge of the octahedron, which connects two Ising spins, is a common edge of two adjacent octahedrons (thin solid lines in Fig. 1). The ensemble of all Ising spins then forms a square lattice, which has a couple of the Heisenberg spins above and below a center of each elementary square face formed by four Ising spins. Let both apical Heisenberg spins interact together via the pairwise *XYZ* Heisenberg interaction, while are also assumed to be engaged in two different quartic Ising interactions with two Ising spins from opposite corners of a square face (see Fig. 1). The total Hamiltonian can be for convenience written as a sum over all elementary unit cells (octahedrons) $\hat{\mathcal{H}}=\Sigma_p\hat{\mathcal{H}}_p$, where each octahedron-cluster Hamiltonian $\hat{\mathcal{H}}_p$ contains one pair interaction between the apical Heisenberg spins and two quartic interactions between the Heisenberg spins and their four Ising neighbors,

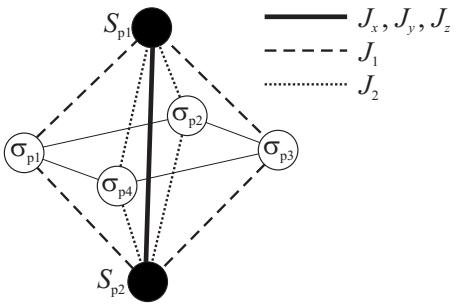

FIG. 1. The elementary unit cell of the spin-1/2 Ising-Heisenberg model. Full (empty) circles denote lattice positions of the Heisenberg (Ising) spins, thick solid line represents the pairwise *XYZ* Heisenberg interaction between the apical Heisenberg spins, and both types of broken lines connect spins involved in the quartic Ising interactions. Thin solid lines connecting four Ising spins are guides for eyes only.

$$\hat{\mathcal{H}}_p = -(J_x\hat{S}^x_{p1}\hat{S}^x_{p2} + J_y\hat{S}^y_{p1}\hat{S}^y_{p2} + J_z\hat{S}^z_{p1}\hat{S}^z_{p2}) - J_1\hat{S}^z_{p1}\hat{S}^z_{p2}\hat{\sigma}^z_{p1}\hat{\sigma}^z_{p3} - J_2\hat{S}^z_{p1}\hat{S}^z_{p2}\hat{\sigma}^z_{p2}\hat{\sigma}^z_{p4}. \quad (1)$$

Above, the interaction parameters J_x, J_y, and J_z denote spatial components of the anisotropic *XYZ* interaction between the Heisenberg spins, while the interaction parameters J_1 and J_2 label two quartic Ising interactions between both apical Heisenberg spins and two Ising spins from opposite corners of a square face along two different diagonal directions (see Fig. 1).

It is of principal importance that the cluster Hamiltonians of two different octahedrons commute with each other, i.e., $[\hat{\mathcal{H}}_i,\hat{\mathcal{H}}_j]=0$, which immediately allows a partial factorization of the total partition function into a product of cluster partition functions,

$$\mathcal{Z} = \sum_{\{\sigma\}}\prod_p \mathrm{Tr}_p \exp(-\beta\hat{\mathcal{H}}_p). \quad (2)$$

The summation $\Sigma_{\{\sigma\}}$ to emerge in Eq. (2) is carried out over all possible configurations of the Ising spins, the symbol Tr_p denotes a trace over spin degrees of freedom of the Heisenberg spin pair from the pth octahedron, and $\beta=1/k_BT$, where k_B is Boltzmann's constant and T is the absolute temperature. After performing the relevant trace over spin degrees of freedom of the Heisenberg spins, the partition function of the Ising-Heisenberg model can be rewritten into the form

$$\mathcal{Z} = \sum_{\{\sigma\}}\prod_p \omega_p(\sigma^z_{p1},\sigma^z_{p2},\sigma^z_{p3},\sigma^z_{p4}). \quad (3)$$

Apparently, the effective Boltzmann's factor ω_p assigned to the pth octahedron now explicitly depends just on four Ising spins σ_{p1}, σ_{p2}, σ_{p3}, and σ_{p4} from its basal plane through the relation

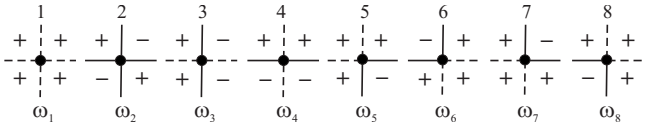

FIG. 2. Eight possible Ising spin configurations and their relation to line coverings of the corresponding eight-vertex model on a dual square lattice. The sign "±" denotes the spin state $\sigma^z = \pm 1/2$.

$$\omega_p(a,b,c,d) = 2\exp(K_z + K_1 ac + K_2 bd)\cosh(K_x - K_y) + 2\exp(-K_z - K_1 ac - K_2 bd)\cosh(K_x + K_y), \tag{4}$$

where we have introduced a new unified notation for the coupling constants $K_\alpha = \beta J_\alpha/4$ $(\alpha = x,y,z,1,2)$ in order to write Boltzmann's factor (4) in a more abbreviated and elegant form.

At this stage, the model under investigation can be rather straightforwardly mapped to the eight-vertex model on its dual square lattice. As a matter of fact, the product emerging in Eq. (3) can alternatively be performed over all elementary squares of the Ising spins forming a square lattice and Boltzmann's factor (4) is invariant under the reversal of all four Ising spin variables. In this respect, there are at the utmost eight different spin arrangements that have different energies (Boltzmann's weights) and these can readily be related to Boltzmann's weights of the eight-vertex model on a dual square lattice by the following procedure. If and only if the Ising spins located at adjacent corners of a square face are aligned opposite to each other, then solid lines are drawn on edges of a dual square lattice; otherwise they are drawn as broken lines. This is actually one of many alternative definitions of the eight-vertex model, since an even number of solid (broken) lines is always incident to each vertex of a dual square lattice. The diagrammatic representation of eight possible spin arrangements and their corresponding line coverings is shown in Fig. 2. It can be easily understood that each of eight possible line arrangements around a vertex of the dual lattice corresponds to two spin configurations, with one obtained from the other by reversing all four Ising spins located at corners of an elementary square face. The hybrid Ising-Heisenberg model thus turns out to be equivalent to the eight-vertex model. With regard to this equivalence, the partition function of the Ising-Heisenberg model can be expressed in terms of the partition function of the eight-vertex model on a square lattice,

$$\mathcal{Z}(T,J_x,J_y,J_z,J_1,J_2) = 2\mathcal{Z}_{8\text{-vertex}}(\omega_1,\omega_2,\ldots,\omega_8). \tag{5}$$

The factor of 2 in the above equation comes from the two-to-one mapping between the spin and vertex configurations (two spin configurations always correspond to one vertex configuration).

Boltzmann's weights, which correspond to eight possible line coverings of the eight-vertex model shown in Fig. 2, can directly be obtained from Eq. (4) by substituting a respective spin configuration of the Ising spins,

$$\omega_1 = \omega_2 = 2\exp\left(K_z + \frac{K_1+K_2}{4}\right)\cosh(K_x - K_y) + 2\exp\left(-K_z - \frac{K_1+K_2}{4}\right)\cosh(K_x + K_y), \tag{6}$$

$$\omega_3 = \omega_4 = 2\exp\left(K_z - \frac{K_1+K_2}{4}\right)\cosh(K_x - K_y) + 2\exp\left(-K_z + \frac{K_1+K_2}{4}\right)\cosh(K_x + K_y), \tag{7}$$

$$\omega_5 = \omega_6 = 2\exp\left(K_z - \frac{K_1-K_2}{4}\right)\cosh(K_x - K_y) + 2\exp\left(-K_z + \frac{K_1-K_2}{4}\right)\cosh(K_x + K_y), \tag{8}$$

$$\omega_7 = \omega_8 = 2\exp\left(K_z + \frac{K_1-K_2}{4}\right)\cosh(K_x - K_y) + 2\exp\left(-K_z - \frac{K_1-K_2}{4}\right)\cosh(K_x + K_y). \tag{9}$$

It is quite obvious from the set of Eqs. (6)–(9) that Boltzmann's weights are pairwise equal to each other and there are merely four independent Boltzmann's weights. The spin-1/2 Ising-Heisenberg model defined through Hamiltonian (1) has been accordingly mapped to the eight-vertex model, which quite generally satisfies Baxter's zero-field condition $\omega_1 = \omega_2$, $\omega_3 = \omega_4$, $\omega_5 = \omega_6$, and $\omega_7 = \omega_8$ [1,28,29]. Hence, it follows that the exact solution of the spin-1/2 Ising-Heisenberg model with the pair *XYZ* Heisenberg interaction and the quartic Ising interactions can be extracted from Baxter's exact solution of the corresponding zero-field eight-vertex model [1,28,29]. For instance, the critical condition of the zero-field eight-vertex model,

$$\omega_1 + \omega_3 + \omega_5 + \omega_7 = 2\max\{\omega_1,\omega_3,\omega_5,\omega_7\}, \tag{10}$$

directly determines phase transitions of the spin-1/2 Ising-Heisenberg model if effective Boltzmann's weights (6)–(9) are substituted into this critical condition. It is also worthy to mention that the critical exponents, which characterize the phase transitions of the zero-field eight-vertex model, continuously change with the parameter $\mu = 2\arctan(\omega_5\omega_7/\omega_1\omega_3)^{1/2}$ by following the formulas

$$\alpha = \alpha' = 2 - \frac{\pi}{\mu}, \quad \beta = \frac{\pi}{16\mu}, \quad \nu = \nu' = \frac{\pi}{2\mu}, \quad \gamma = \gamma' = \frac{7\pi}{8\mu}, \quad \delta = 15, \quad \eta = \frac{1}{4}. \tag{11}$$

Note that set of relations (11) will also govern changes in the critical exponents of the Ising-Heisenberg model provided that effective Boltzmann's weights (6)–(9) are used for the calculation of the parameter μ.

To provide an alternative proof of the exact mapping equivalence between the zero-field eight-vertex model and

the spin-1/2 Ising-Heisenberg model, one can utilize the fact that the eight-vertex model on a square lattice can also be reformulated as two spin-1/2 Ising square lattices coupled together by means of the quartic interaction [26,27]. In accordance with this statement, effective Boltzmann's factor (4) could be eventually replaced via appropriate algebraic transformation of the form

$$\begin{aligned}\omega_p(\sigma_{p1}^z,\sigma_{p2}^z,\sigma_{p3}^z,\sigma_{p4}^z) &= 2\exp(K_z+K_1\sigma_{p1}^z\sigma_{p3}^z+K_2\sigma_{p2}^z\sigma_{p4}^z)\cosh(K_x-K_y)\\ &\quad+2\exp(-K_z-K_1\sigma_{p1}^z\sigma_{p3}^z-K_2\sigma_{p2}^z\sigma_{p4}^z)\cosh(K_x+K_y)\\ &= R_0\exp(R_1\sigma_{p1}^z\sigma_{p3}^z+R_2\sigma_{p2}^z\sigma_{p4}^z+R_4\sigma_{p1}^z\sigma_{p2}^z\sigma_{p3}^z\sigma_{p4}^z),\end{aligned} \tag{12}$$

where the mapping parameters R_1 and R_2 denote the effective pair interactions in two different Ising square lattices and the mapping parameter R_4 determines the effective quartic interaction that couples together both Ising square lattices. Algebraic transformation (12) must satisfy the "self-consistency" condition, which means that it must hold independently of spin states of four Ising spins involved therein. The self-consistency condition thus provides a simple connection between effective Boltzmann's weights (6)–(9) of the Ising-Heisenberg model and the coupling parameters R_1, R_2, and R_4 of the zero-field eight-vertex model in the Ising representation,

$$R_0=(\omega_1\omega_3\omega_5\omega_7)^{1/4}, \tag{13}$$

$$R_1=\ln\left(\frac{\omega_1\omega_7}{\omega_3\omega_5}\right), \tag{14}$$

$$R_2=\ln\left(\frac{\omega_1\omega_5}{\omega_3\omega_7}\right), \tag{15}$$

$$R_4=4\ln\left(\frac{\omega_1\omega_3}{\omega_5\omega_7}\right). \tag{16}$$

This is actually an alternative proof of the exact mapping equivalence between the spin-1/2 Ising-Heisenberg model and the zero-field eight-vertex model on a square lattice.

The usefulness of the latter equivalence consists in that another three useful observations can be made from it. First, it is quite evident from Eqs. (14) and (15) that the effective pair interactions of both Ising square lattices become equal to each other ($R_1=R_2$) by imposing the condition $\omega_5=\omega_7$, which is equivalent to $K_1=K_2$ (or $J_1=J_2$). This means that a difference in two diagonal quartic Ising interactions merely causes a difference in the effective pair interactions of the Ising square lattices. Second, the quartic interaction R_4 that couples together two Ising square lattices vanishes only if at least one from either of quartic Ising interaction K_1 or K_2 (J_1 or J_2) equals zero provided that all interactions are finite. Other particular cases with the zero effective quartic interaction R_4 are the Ising and XY limit of the Heisenberg pair interaction. One actually obtains $R_4\to 0$, $R_1\to\pm K_1$, and $R_2\to\pm K_2$ in the Ising limit $K_z\to\pm\infty$, whereas $R_4\to 0$, $R_1\to -K_1$, and $R_2\to -K_2$ is obtained in the XY limit K_x, $K_y\to\pm\infty$. Apart from these rather trivial cases from the Ising universality class, one may expect that the spin-1/2 Ising-Heisenberg model will generally exhibit continuously varying critical exponents satisfying the weak universality hypothesis [60] due to the nonzero effective quartic interaction R_4. Third, the spin-1/2 Ising-Heisenberg model defined through Hamiltonian (1) can in turn be refined by the terms depending on the Ising spin pairs $\sigma_{p1}^z\sigma_{p3}^z$ and $\sigma_{p2}^z\sigma_{p4}^z$ without disturbing the exact mapping equivalence to the zero-field eight-vertex model. As a matter of fact, an inclusion of two diagonal pair interactions $-J_1'\sigma_{p1}^z\sigma_{p3}^z$ and $-J_2'\sigma_{p2}^z\sigma_{p4}^z$, and the quartic interaction $-J_4'\sigma_{p1}^z\sigma_{p2}^z\sigma_{p3}^z\sigma_{p4}^z$ into Hamiltonian (1) merely adds the respective coupling constant as an auxiliary constant factor into the definition of mapping parameters (14)–(16), respectively. It is noteworthy, however, that the model system is mapped to the more general and yet unsolved eight-vertex model by introducing the nearest-neighbor pair interactions $-J_1''(\sigma_{p1}^z\sigma_{p2}^z+\sigma_{p3}^z\sigma_{p4}^z)$ and $-J_2''(\sigma_{p2}^z\sigma_{p3}^z+\sigma_{p1}^z\sigma_{p4}^z)$ into Hamiltonian (1). Even though there does not exist a general exact solution of the corresponding eight-vertex model, it is now well established that the critical exponents still vary continuously with the interaction parameters even for this more complex but surely more realistic model [61–70].

III. RESULTS AND DISCUSSION

Before proceeding to a discussion of the most interesting results, it is worthy to notice that our further analysis will be restricted just to a particular example of the spin-1/2 Ising-Heisenberg model with the identical quartic Ising interactions $J_1=J_2=J_4$ and the more symmetric XXZ Heisenberg interaction with $J_x=J_y=J\Delta$ and $J_z=J$ in order to avoid over parametrization of the model under investigation. Furthermore, it is also convenient to normalize all interaction parameters with respect to the z component of the XXZ Heisenberg interaction, which will henceforth serve as the energy unit. Accordingly, the dimensionless temperature will be set to k_BT/J, the relative strength of the quartic Ising interactions will be proportional to the ratio J_4/J, and, finally, the parameter $\Delta=J_x/J=J_y/J$ will measure the relative strength of the exchange anisotropy in the XXZ Heisenberg interaction.

Let us perform first a comprehensive analysis of the ground state. It is worthwhile to remark that the ground-state spin arrangement will be thoroughly determined by the lowest-energy eigenstate that enters into the greatest Boltzmann's weight, since each Boltzmann's weight involves four eigenenergies that correspond to possible eigenstates of the Heisenberg spin pair at a given configuration of the Ising spins. (Remember that the Ising spin configurations are unambiguously assigned to Boltzmann's weights according to a scheme depicted in Fig. 2.) It might be therefore quite useful to quote initially explicit expressions for the effective Boltzmann's weights of simplified version of the spin-1/2 Ising-Heisenberg model,

$$\omega_1=2\exp\left[\frac{\beta(2J+J_4)}{8}\right]+2\exp\left[-\frac{\beta(2J+J_4)}{8}\right]\cosh\left(\frac{\beta J\Delta}{2}\right),$$

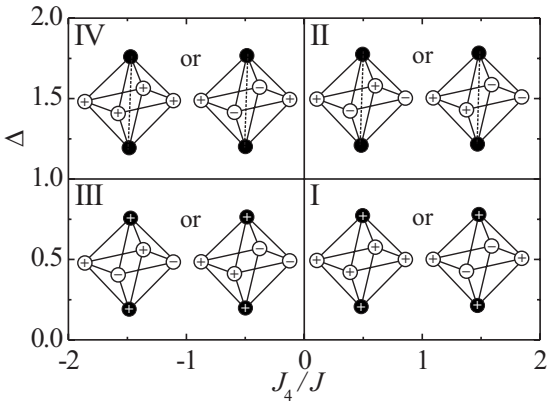

FIG. 3. Ground-state phase diagram of the spin-1/2 Ising-Heisenberg model with the ferromagnetic interaction $J>0$ in the J_4/J-Δ plane. Each sector of the phase diagram contains typical spin configurations of the Ising and Heisenberg spins, which form an elementary octahedron. The sign "$\pm$" denotes spin states $\sigma^z = \pm 1/2$ and $S^z = \pm 1/2$ of the Ising and Heisenberg spins, respectively. Broken lines, which connect both apical Heisenberg spins in phases $|\mathrm{II}\rangle$ and $|\mathrm{IV}\rangle$, label the entangled spin state $(|+,-\rangle+|-,+\rangle)/\sqrt{2}$.

$$\omega_3 = 2\exp\left[\frac{\beta(2J-J_4)}{8}\right] + 2\exp\left[-\frac{\beta(2J-J_4)}{8}\right]\cosh\left(\frac{\beta J\Delta}{2}\right),$$

$$\omega_5 = \omega_7 = 2\exp\left(\frac{\beta J}{4}\right) + 2\exp\left(-\frac{\beta J}{4}\right)\cosh\left(\frac{\beta J\Delta}{2}\right). \tag{17}$$

It directly follows from set of equations (17) that the greatest Boltzmann's weight is either ω_1 or ω_3. Moreover, another useful observation is that both these Boltzmann's weights are simply connected through the relation $\omega_1(\pm J_4)=\omega_3(\mp J_4)$ and one may further assume the positive quartic Ising interaction $J_4>0$ without loss of generality. This simplification is a direct consequence of the affirmation that the investigated model system is invariant under the transformations $J_4 \to -J_4$ and $(\sigma^z_{p1},\sigma^z_{p2},\sigma^z_{p3},\sigma^z_{p4}) \to (\sigma^z_{p1},\sigma^z_{p2},-\sigma^z_{p3},-\sigma^z_{p4})$. The ground-state phase diagram must be therefore symmetric with respect to the $J_4=0$ axis and the respective spin arrangements to emerge in a sector $J_4<0$ can be obtained from its symmetry-related counterpart in a sector $J_4>0$ by a mere interchange of the Ising spin configurations inherent to Boltzmann's weights ω_1 and ω_3.

For better orientation, we will distinguish our subsequent analysis of the spin-1/2 Ising-Heisenberg models with the ferromagnetic ($J>0$) and antiferromagnetic ($J<0$) Heisenberg pair interactions, respectively. In the former case, the greatest Boltzmann's weight is ω_1 for $\Delta<1$ and ω_3 for $\Delta>1$, under the assumptions $T=0$ and $J_4>0$ (note that the reverse conditions hold for the case $J_4<0$). The global ground-state phase diagram of the spin-1/2 Ising-Heisenberg model with the ferromagnetic Heisenberg interaction is displayed in Fig. 3. Clearly, the ground-state diagram comprises four different phases,

$$|\mathrm{I}\rangle = \prod_p |+,\pm,+,\pm\rangle_{\sigma_p}|+,+\rangle_{S_p}, \tag{18}$$

$$|\mathrm{II}\rangle = \prod_p |+,\pm,-,\mp\rangle_{\sigma_p}\frac{1}{\sqrt{2}}(|+,-\rangle+|-,+\rangle)_{S_p}, \tag{19}$$

$$|\mathrm{III}\rangle = \prod_p |+,\pm,-,\mp\rangle_{\sigma_p}|+,+\rangle_{S_p}, \tag{20}$$

$$|\mathrm{IV}\rangle = \prod_p |+,\pm,+,\pm\rangle_{\sigma_p}\frac{1}{\sqrt{2}}(|+,-\rangle+|-,+\rangle)_{S_p}, \tag{21}$$

which are written in the form of the product over the respective lowest-energy eigenstate of Hamiltonian (1) that is of course identical for each elementary unit cell (octahedron). Note furthermore that the first (second) ket vector after the product symbol determines spin states of the Ising (Heisenberg) spins and another equivalent representations of the eigenstates can be obtained from eigenvectors (18)–(21) under the reversal of all Ising and/or Heisenberg spins. Phases $|\mathrm{I}\rangle$ and $|\mathrm{III}\rangle$ are consequently eightfold degenerate as spin reversals of the Ising and Heisenberg spins can be performed independently of each other, whereas phases $|\mathrm{II}\rangle$ and $|\mathrm{IV}\rangle$ are just fourfold degenerate as the spin reversal of the Heisenberg spins does not in fact lead to a new eigenstate.

It is worthwhile to remark that another two obvious features directly follow from Fig. 3 and Eqs. (18)–(21). The Heisenberg spins are ferromagnetically aligned with respect to each other in phases $|\mathrm{I}\rangle$ and $|\mathrm{III}\rangle$ where $\Delta<1$, while they reside at the entangled spin state $(|+,-\rangle+|-,+\rangle)/\sqrt{2}$ in phases $|\mathrm{II}\rangle$ and $|\mathrm{IV}\rangle$ where $\Delta>1$. In addition, there appears a perfect ferromagnetic or antiferromagnetic alignment on a square lattice of the Ising spins in phases $|\mathrm{I}\rangle$ and $|\mathrm{IV}\rangle$ in contrast to two feasible superantiferromagnetic orderings that occur in phases $|\mathrm{II}\rangle$ and $|\mathrm{III}\rangle$, where a perfect ferromagnetic arrangement of the Ising spins in a horizontal direction is accompanied with a perfect antiferromagnetic arrangement in a vertical direction, or vice versa. The overall understanding of the nature of the afore-described spin arrangements readily follows from the energy spectrum of the spin-1/2 *XXZ* Heisenberg dimer. Namely, the lowest-energy eigenstate of the spin-1/2 *XXZ* Heisenberg dimer is the ferromagnetic state $|+,+\rangle$ if one considers the easy-axis exchange anisotropies $\Delta<1$, while the entangled spin state $(|+,-\rangle+|-,+\rangle)/\sqrt{2}$ becomes the lowest-energy eigenstate for the easy-plane exchange anisotropies $\Delta>1$. The relevant spin arrangement of the Ising spins is subsequently driven by the effort to minimize the energy gain arising from the quartic Ising interactions. Thus, there must be either zero or two spins with opposite orientation with respect to the others among the four spins (two Ising and two Heisenberg) involved in the positive quartic Ising interaction $J_4>0$, whereas there must be just one unaligned spin among them whenever the negative quartic Ising interaction $J_4<0$ is assumed.

Surprisingly, the ground-state analysis becomes much simpler for the spin-1/2 Ising-Heisenberg model with the antiferromagnetic ($J<0$) Heisenberg interaction. It is quite apparent from set of equations (17) that the greatest Boltz-

mann's weight is always ω_3 (ω_1) if one considers the positive (negative) quartic Ising interaction. Owing to this fact, the overall ground-state phase diagram comprises just two different phases,

$$|\mathrm{V}\rangle = \prod_p |+,\pm,-,\mp\rangle_{\sigma_p} \frac{1}{\sqrt{2}}(|+,-\rangle - |-,+\rangle)_{S_p}, \quad (22)$$

$$|\mathrm{VI}\rangle = \prod_p |+,\pm,+,\pm\rangle_{\sigma_p} \frac{1}{\sqrt{2}}(|+,-\rangle - |-,+\rangle)_{S_p}, \quad (23)$$

whereas phase $|\mathrm{V}\rangle$ is the ground state for $J_4>0$ and phase $|\mathrm{VI}\rangle$ is that for $J_4<0$. It should be stressed that both fourfold-degenerate phases $|\mathrm{V}\rangle$ and $|\mathrm{VI}\rangle$ quite closely resemble phases $|\mathrm{II}\rangle$ and $|\mathrm{IV}\rangle$ described previously by the analysis of the ferromagnetic model. As a matter of fact, the only difference between phases $|\mathrm{V}\rangle$ and $|\mathrm{II}\rangle$ (or $|\mathrm{VI}\rangle$ and $|\mathrm{IV}\rangle$) consists of a quantum entanglement of the Heisenberg spin pairs, which is described by the antisymmetric singlet-dimer wave function $(|+,-\rangle-|-,+\rangle)/\sqrt{2}$ in the antiferromagnetic model with $J<0$ and its symmetric counterpart $(|+,-\rangle+|-,+\rangle)/\sqrt{2}$ in the ferromagnetic model with $J>0$.

Now, let us turn our attention to a detailed analysis of the finite-temperature phase diagrams. It is worthwhile to recall that phase-transition lines of our simplified version of the spin-1/2 Ising-Heisenberg model can be straightforwardly obtained from the critical condition of the corresponding zero-field eight-vertex model by substituting effective Boltzmann's weights (17) into Eq. (10). It should be also mentioned that the greatest Boltzmann's weight might be either ω_1 or ω_3. In the former case ($\omega_1>\omega_3$), the critical condition reads

$$\cosh\left(\frac{\beta_c J}{2}\Delta\right) = \exp\left(\frac{\beta_c J}{2}\right)\frac{\sinh\left(\frac{\beta_c J_4}{8}\right)-1}{\sinh\left(\frac{\beta_c J_4}{8}\right)+1}, \quad (24)$$

while in the latter case ($\omega_1<\omega_3$) the critical condition becomes

$$\cosh\left(\frac{\beta_c J}{2}\Delta\right) = \exp\left(\frac{\beta_c J}{2}\right)\frac{\sinh\left(\frac{\beta_c J_4}{8}\right)+1}{\sinh\left(\frac{\beta_c J_4}{8}\right)-1}, \quad (25)$$

where $\beta_c = 1/k_B T_c$ and T_c is the critical temperature. Interestingly, both critical conditions (24) and (25) can be joined together to yield a single critical condition,

$$\sinh\left(\frac{\beta_c |J_4|}{8}\right) = \frac{\exp\left(\frac{\beta_c J}{2}\right)+\cosh\left(\frac{\beta_c J}{2}\Delta\right)}{\left|\exp\left(\frac{\beta_c J}{2}\right)-\cosh\left(\frac{\beta_c J}{2}\Delta\right)\right|}, \quad (26)$$

which is valid in the whole region of the parameter space. The absolute value of the quartic Ising interaction appears in Eq. (26) as a direct consequence of the symmetry relation between Boltzmann's weights, $\omega_1(\pm J_4)=\omega_3(\mp J_4)$, which are mutually interchangeable under the transformation $J_4 \to -J_4$. Accordingly, the critical temperature of the spin-1/2 Ising-Heisenberg model must be independent of the sign of the quartic Ising interaction and one may still consider positive values of the quartic Ising interaction $J_4>0$ without loss of generality. Henceforth, we will therefore restrict ourselves just to an analysis of the critical lines of phases $|\mathrm{I}\rangle$, $|\mathrm{II}\rangle$, and $|\mathrm{V}\rangle$ emerging for the positive quartic Ising interaction $J_4>0$. It should be nevertheless mentioned that the critical lines for phases $|\mathrm{III}\rangle$, $|\mathrm{IV}\rangle$, and $|\mathrm{VI}\rangle$ appearing in the case $J_4<0$ are formally identical with the displayed critical lines for phases $|\mathrm{I}\rangle$, $|\mathrm{II}\rangle$, and $|\mathrm{V}\rangle$, respectively.

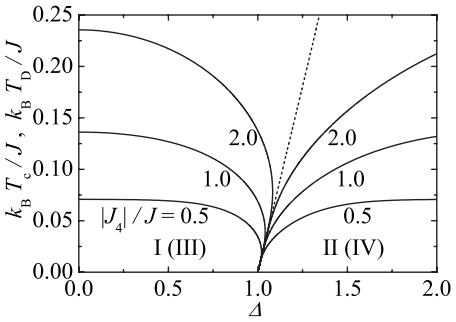

FIG. 4. Solid lines depict the critical temperature as a function of the exchange anisotropy for the spin-1/2 Ising-Heisenberg model with the ferromagnetic Heisenberg interaction $J>0$ at three different relative strengths of the quartic Ising interaction. The left wing of critical lines determines phase boundaries for phases $|\mathrm{I}\rangle$ ($J_4>0$) or $|\mathrm{III}\rangle$ ($J_4<0$), while the right wing determines phase boundaries for phases $|\mathrm{II}\rangle$ ($J_4>0$) or $|\mathrm{IV}\rangle$ ($J_4<0$). The broken line shows the disorder solution obtained by solving Eq. (28).

Let us construct first the finite-temperature phase diagram of the spin-1/2 Ising-Heisenberg model with the ferromagnetic Heisenberg interaction. The greatest Boltzmann's weight for the ferromagnetic model with $J>0$ is ω_1 if and only if

$$\mathrm{sgn}(J_4)\left[\exp\left(\frac{\beta J}{2}\right)-\cosh\left(\frac{\beta J}{2}\Delta\right)\right] > 0. \quad (27)$$

Otherwise ω_3 becomes the greatest Boltzmann's weight. Consequently, critical condition (24) determines phase transitions just if inequality (27) holds, while critical condition (25) is valid in the rest of the parameter space. Phase-transition lines in the form of critical temperature versus exchange anisotropy dependences are drawn in Fig. 4 for three different relative strengths of the quartic Ising interaction. As one can see, the critical temperature generally exhibits a remarkable dependence on the exchange anisotropy with two marked wings of critical lines that merge together at the ground-state boundary $\Delta=1$ between phases $|\mathrm{I}\rangle$ and $|\mathrm{II}\rangle$. It should be mentioned that the left wing of displayed phase boundaries is a solution of critical condition (24), while the right wing is a solution of critical condition (25). In this regard, the left wings deliminate critical lines of phase $|\mathrm{I}\rangle$, whereas the right wings represent critical lines of phase $|\mathrm{II}\rangle$. The critical temperature of phase $|\mathrm{I}\rangle$ at first steadily decreases as the exchange anisotropy Δ is raised from zero,

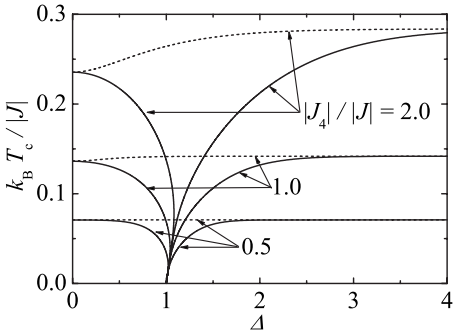

FIG. 5. The critical temperature as a function of the exchange anisotropy for the spin-1/2 Ising-Heisenberg model with the ferromagnetic (solid lines) or antiferromagnetic (broken lines) Heisenberg pair interaction at three different relative strengths of the quartic Ising interaction.

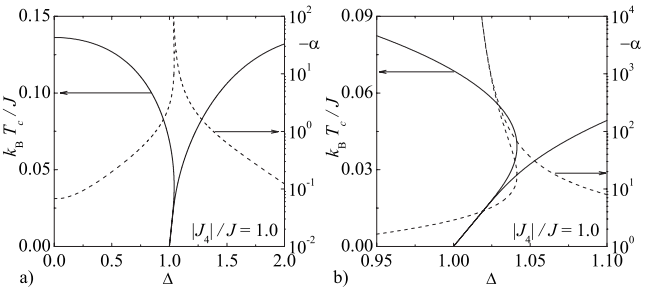

FIG. 6. The changes in the critical exponent α along the critical line of the spin-1/2 Ising-Heisenberg model with the ferromagnetic interaction $J>0$ and $|J_4|/J=1.0$. Solid lines, which are scaled with respect to left axes, show the critical temperature as a function of the exchange anisotropy. Broken lines, which are scaled with respect to right axes, display the relevant changes in the critical exponent $-\alpha$ in a semilogarithmic scale. (b) illustrates a detail of the parameter region, where both re-entrant phase transitions as well as a quantum critical point occur.

then it exhibits an interesting re-entrant behavior before it finally tends to zero in the limit $\Delta \to 1$. It is noticeable that the re-entrant phase transitions are observable just in a relatively narrow interval of the exchange anisotropies $\Delta \in (1, \Delta_{\max})$, whose upper bound $\Delta_{\max}$ is the greater the greater is the relative strength of the quartic Ising interaction. Contrary to this, the right wing of critical lines, which allocate phase transitions of phase $|\mathrm{II}\rangle$, characterizes a monotonous increase in the critical temperature with the exchange anisotropy. An origin of the observed re-entrant transitions obviously lies in two times higher degeneracy of phase $|\mathrm{I}\rangle$ compared to phase $|\mathrm{II}\rangle$. Accordingly, two successive re-entrant transitions from the paramagnetic phase to phase $|\mathrm{I}\rangle$ and back may take place in the parameter region, where phase $|\mathrm{II}\rangle$ constitutes the ground state and phase $|\mathrm{I}\rangle$ has slightly higher energy, on account of the much larger entropy gain of phase $|\mathrm{I}\rangle$ obtained upon the temperature increase. It is worthy to mention that similar re-entrant phase transitions have been found in a variety of frustrated Ising models, which have been exactly solved by establishing a precise mapping relationship with the corresponding free-fermion vertex models [2,71–76]. To bring a deeper insight into the re-entrant phenomenon, it is also worthwhile to inspect the disorder solution to be derived from the condition

$$\omega_1 = \omega_3 \Leftrightarrow \exp\left(\frac{\beta_D J}{2}\right) = \cosh\left(\frac{\beta_D J \Delta}{2}\right), \tag{28}$$

where $\beta_D = 1/k_B T_D$ and T_D is the disorder temperature. The disorder solution entails an effective reduction in the dimensionality and ensures a disordered nature of the spin system on the particular subvariety of the parameter space given by Eq. (28) [2,73–79]. It is quite apparent from Fig. 4 that the disorder (broken) line calculated from condition (28) has a finite positive tangent, which can be approximated in a relatively wide temperature range by the linear dependence of the disorder temperature T_D on the exchange anisotropy Δ through the relation $k_B T_D / J = (\Delta - 1)/\ln 4$.

For the sake of comparison, the critical temperatures of the spin-1/2 Ising-Heisenberg model with both ferromagnetic ($J>0$) and antiferromagnetic ($J<0$) Heisenberg pair interactions are depicted in Fig. 5 for three different relative strengths of the quartic Ising interaction. The critical lines of the ferromagnetic model are displayed as solid lines, while the critical lines of the antiferromagnetic model are drawn as broken lines. The displayed critical lines of the antiferromagnetic model in fact determine critical temperatures of phase $|\mathrm{V}\rangle$, which is the only possible ground state when $J<0$ and $J_4>0$. Evidently, the antiferromagnetic model generally exhibits a rather small variation in the critical temperature upon varying the exchange anisotropy in comparison with the marked two-wing dependence of the critical temperature that shows the ferromagnetic model. Another interesting fact to observe here, and also derived from Eq. (26), is that the critical temperatures of the ferromagnetic and antiferromagnetic models become equal to each other in two limiting cases $\Delta \to 0$ and $\Delta \to \infty$. From this perspective, the most obvious difference between the critical temperatures of the ferromagnetic and antiferromagnetic Ising-Heisenberg models appears in the vicinity of the isotropic limit $\Delta = 1$, where the critical temperature of the ferromagnetic model asymptotically vanishes due to the zero-temperature phase transition between phases $|\mathrm{I}\rangle$ and $|\mathrm{II}\rangle$.

At this point, let us make certain comments on changes in critical exponents along the critical lines. For this purpose, typical changes in the critical exponent α along the phase-transition line of the spin-1/2 Ising-Heisenberg model with the ferromagnetic Heisenberg interaction and $|J_4|/J=1$ are depicted in Fig. 6. Solid lines display the variation in the critical temperature with the exchange anisotropy, which are scaled with respect to left axes, while broken lines scaled with respect to right axes show the relevant changes in the critical exponent α. As could be expected, the critical exponent α varies continuously along the line of critical points according to relations (11), which connect changes in the critical exponents to respective changes in the interaction parameters through the parameter μ. It turns out that the investigated model system generally exhibits rather smooth continuous phase transitions, since the order of phase transition is proportional to $r = 2 - \alpha$ (see, for instance, pp. 16 and 17 of Ref. [1]) and the critical exponent α lies within the range $\alpha \in (-\infty, 0)$. The most striking finding is, however, that

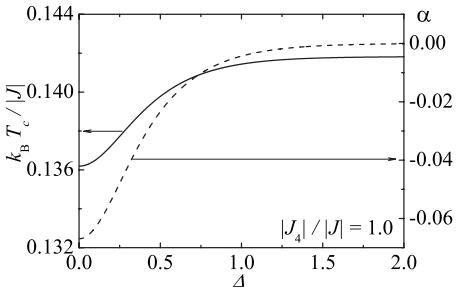

FIG. 7. The changes in the critical exponent α along the critical line of the spin-1/2 Ising-Heisenberg model with the antiferromagnetic interaction $J<0$ and $|J_4|/|J|=1.0$. The solid line, which is scaled with respect to the left axis, shows the critical temperature as a function of the exchange anisotropy. The broken line, which is scaled with respect to the right axis, displays the relevant changes in the critical exponent α along this critical line.

the critical exponent α exhibits a peculiar singularity in the vicinity of the ground-state boundary between phases $|\mathrm{I}\rangle$ and $|\mathrm{II}\rangle$ where $\alpha\to-\infty$. Owing to this fact, the zero-temperature phase transition between phases $|\mathrm{I}\rangle$ and $|\mathrm{II}\rangle$ emerging at $\Delta=1$ is of infinite order. Hence, this special critical point actually represents a remarkable quantum critical point. It is also worthy to notice that the displayed variations in the critical exponent $-\alpha$ quite closely resemble dependences of the other critical exponents β, γ, and ν due to a similar mathematical structure of relations (11).

Furthermore, the changes in the critical exponent α along the critical line of the spin-1/2 Ising-Heisenberg model with the antiferromagnetic Heisenberg interaction are shown in Fig. 7. In this particular case, the changes in the critical exponent α are restricted to a rather narrow finite interval even though a negative value of the critical exponent α still implies the continuous nature of the phase transitions $r\geq 2$. It is also quite interesting to notice that the critical exponent α monotonically increases from its smallest value at $\Delta=0$ before it gradually tends toward $\alpha\to 0$ in the limit $\Delta\to\infty$. Altogether, the critical lines of both ferromagnetic and antiferromagnetic models turned out to be the lines of continuous phase transitions of the order $r\geq 2$, but the ferromagnetic model generally exhibits much more pronounced changes in the critical exponents including a rather strange quantum critical point of the infinite order with diverging critical exponents.

Before concluding, let us make few remarks on a critical behavior of another particular case of the spin-1/2 Ising-Heisenberg model with $J_x=J_y=J\Delta$ and $J_z=J$ and the quartic Ising interactions $J_1=-J_2=J_4'$. This particular case differs from the previous one just in a nature of the quartic Ising interactions, which are of equal relative strengths but of different signs. In this respect, the positive quartic interaction will prefer spin alignments with either zero or two opposite spins among the four spins (two Ising and two Heisenberg) involved therein, while the negative quartic interaction will favor spin alignments with just one unaligned spin among them. Interestingly, the phase diagrams of this particular case will be essentially identical to the ones discussed previously, since there is a simple relation between the effective Boltzmann's weights of both particular cases. As a matter of fact, it directly follows from Eqs. (6)–(9) that the effective Boltzmann's weights of the model with two nonuniform quartic interactions $J_1=-J_2=J_4'$ can be expressed through Boltzmann's weights (17) of the uniform case as $\omega_1'=\omega_3'=\omega_5$, $\omega_5'=\omega_3$, and $\omega_7'=\omega_1$. It is quite apparent that the roles of different Boltzmann's weights are merely interchanged and the greatest Boltzmann's weight is now either ω_7' or ω_5'. However, this fact does not affect the ground-state and finite-temperature phase diagrams because critical condition (10) is quite symmetric with respect to all four Boltzmann's weights involved therein. Hence, it follows that the zero- and finite-temperature phase diagrams shown in Figs. 3–5 remain valid and one should only perform a respective change in the Ising spin configurations from $\omega_1\to\omega_7'$ and $\omega_3\to\omega_5'$, respectively. The ground-state phase diagram of the ferromagnetic ($J>0$) model with the nonuniform quartic interactions, which is shown in Fig. 3, thus constitute the phases

$$|\mathrm{I}'\rangle=\prod_p|+,\mp,+,\pm\rangle_{\sigma_p}|+,+\rangle_{S_p}, \tag{29}$$

$$|\mathrm{II}'\rangle=\prod_p|\pm,+,\mp,+\rangle_{\sigma_p}\frac{1}{\sqrt{2}}(|+,-\rangle+|-,+\rangle)_{S_p}, \tag{30}$$

$$|\mathrm{III}'\rangle=\prod_p|\pm,+,\mp,+\rangle_{\sigma_p}|+,+\rangle_{S_p}, \tag{31}$$

$$|\mathrm{VI}'\rangle=\prod_p|+,\mp,+,\pm\rangle_{\sigma_p}\frac{1}{\sqrt{2}}(|+,-\rangle+|-,+\rangle)_{S_p}. \tag{32}$$

while the ground state of the antiferromagnetic ($J<0$) model is either $|\mathrm{V}'\rangle$ for $J_4'>0$ or $|\mathrm{VI}'\rangle$ for $J_4'<0$,

$$|\mathrm{V}'\rangle=\prod_p|\pm,+,\mp,+\rangle_{\sigma_p}\frac{1}{\sqrt{2}}(|+,-\rangle-|-,+\rangle)_{S_p}, \tag{33}$$

$$|\mathrm{VI}'\rangle=\prod_p|+,\mp,+,\pm\rangle_{\sigma_p}\frac{1}{\sqrt{2}}(|+,-\rangle-|-,+\rangle)_{S_p}. \tag{34}$$

Despite similarity of the ground-state and finite-temperature phase diagrams, the critical exponents of the particular case with the nonuniform quartic interactions are fundamentally different from the ones of the former particular case with two identical quartic interactions. Namely, the change in the critical exponents depends through set of equations (11) on the parameter μ, which is not symmetric with respect to all four Boltzmann's weights. Therefore, it might be quite interesting to ascertain how the critical exponents change by assuming two quartic interactions of different sign (nature). The variations in the critical exponent α along the critical line of the ferromagnetic model ($J>0$) are displayed in Fig. 8 for the particular case with $|J_4'|/J=1$. It is quite obvious from this figure that the critical exponent α exhibits an outstanding dependence with the global maximum $\alpha_{\max}=1$ emerging at $\Delta=1$. As a result, the zero-temperature phase transition between phases $|\mathrm{I}'\rangle$ and $|\mathrm{II}'\rangle$ (or $|\mathrm{III}'\rangle$ and $|\mathrm{IV}'\rangle$) is in fact a discontinuous first-order phase transition ($r=1$) unlike the afore-described continuous phase transition of the infinite order between the phases $|\mathrm{I}\rangle$ and $|\mathrm{II}\rangle$ (or $|\mathrm{III}\rangle$ and $|\mathrm{IV}\rangle$). More-

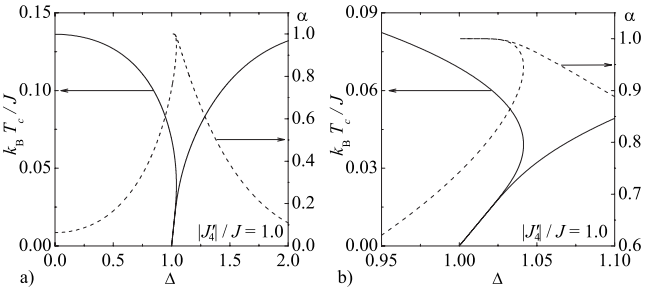

FIG. 8. The changes in the critical exponent α along the critical line of the spin-1/2 Ising-Heisenberg model with the ferromagnetic interaction $J>0$ and the relative strength of the nonuniform quartic interactions $|J_4'|/J=1.0$. Solid lines, which are scaled with respect to left axes, show the critical temperature as a function of the exchange anisotropy. Broken lines, which are scaled with respect to right axes, display the relevant changes in the critical exponent α.

over, the critical exponent α evidently acquires positive values from the interval $\alpha \in (0,1)$, which indicates discontinuous nature of the phase transitions $(r<2)$ along the whole critical line of the ferromagnetic model with the nonuniform quartic interactions.

For completeness, we depict in Fig. 9 the critical exponent α of the antiferromagnetic model $(J<0)$ with the same relative strength of nonuniform quartic interactions $|J_4'|/|J|=1$. It can be clearly seen from this figure that the critical exponent α monotonically decreases with the increase in the exchange anisotropy even although it always remains positive. It is noteworthy that the precisely opposite trends were observed in the former particular case with the uniform quartic interactions and there are only two common features of both particular cases with the antiferromagnetic pair interaction $J<0$. First, the changes in the critical exponent α are restricted just to a rather narrow finite interval and, second, the same asymptotic value $\alpha=0$ is achieved in the limit $\Delta \to \infty$. Altogether, it could be concluded that the Ising-Heisenberg model with the nonuniform quartic interactions generally exhibits a discontinuous phase transitions of the order $r<2$ no matter whether the ferromagnetic or antiferromagnetic nature of the Heisenberg pair interaction J is assumed.

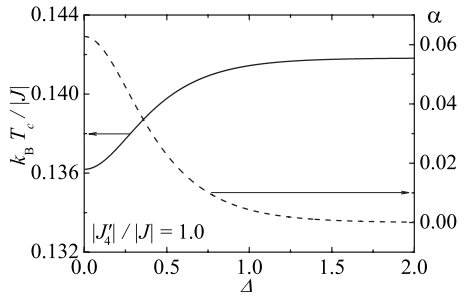

FIG. 9. The changes in the critical exponent α along the critical line of the spin-1/2 Ising-Heisenberg model with the antiferromagnetic interaction $J<0$ and the relative strength of the nonuniform quartic interactions $|J_4'|/|J|=1.0$. The solid line, which is scaled with respect to the left axis, shows the critical temperature as a function of the exchange anisotropy. The broken line, which is scaled with respect to the right axis, displays the relevant changes in the critical exponent α.

IV. CONCLUSIONS

In the present work, we have furnished proof of an exact mapping equivalence between the spin-1/2 Ising-Heisenberg model on a two-dimensional lattice of edge-sharing octahedrons and the zero-field eight-vertex model on a square lattice. In accordance with this exact mapping correspondence, the critical behavior of the model under investigation closely resembles the outstanding critical behavior of the zero-field eight-vertex model and Ashkin-Teller model [1], which exhibit critical lines with continuously varying critical exponents satisfying the weak universality hypothesis [60]. It is worthwhile to remark, moreover, that the similar precise mapping relationship between the spin-1/2 Ising-Heisenberg model on a square-hexagon lattice and the zero-field eight-vertex model was recently found by Valverde [80] *et al.* in a restricted region of the interaction parameters. Unlike this case, the exact mapping correspondence with the zero-field eight-vertex model holds in our case quite generally; i.e., it is not restricted to any particular subvariety of the parameter space.

Exact results for the spin-1/2 Ising-Heisenberg model with the pair *XYZ* Heisenberg and quartic Ising interactions imply that the model with the antiferromagnetic pair interaction surprisingly exhibits less significant changes in both critical temperatures and critical exponents than the model with the ferromagnetic pair interaction. The most interesting finding to emerge from the present study is however exact evidence of a quantum critical point of the infinite order, which characterizes the peculiar singular behavior of the critical exponents in the close vicinity of the isotropic limit of the Heisenberg pair interaction. In addition, it was shown that the critical exponents vary continuously over the entire range of allowed values by changing the exchange anisotropy in the Heisenberg pair interaction and the relative strength of the quartic interaction. From this point of view, the investigated Ising-Heisenberg model represents a rare example of the exactly solved quantum spin model with such an unusual weak universal critical behavior.

Next, it is worth noticing that the Ising-Heisenberg model with the pair Heisenberg and quadratic Ising interactions can also be interpreted as an interesting example of the exactly solved quantum dimer system with rather complicated even-body interactions between dimers. This means that the system of quantum dimers in some specific fluctuations or fields is also equivalent to the exactly solved zero-field eight-vertex model, which contradicts the standard universality hypothesis in that its critical exponents vary continuously with the interaction parameters. In addition, the quartic and other even-body interactions turned out to play an important role in determining magnetic properties of several insulating magnetic materials [32–39], which makes the presented exact results more interesting also from the experimental point of view. Even though it would be rather striking coincidence if some real magnetic material would obey very specific topological requirements of the model under investigation, it is

quite reasonable to suspect that our exact results might at least shed light on some important aspects of the critical behavior of real magnetic materials.

Last but not the least, it should be mentioned that it could be quite interesting to explore also temperature variations of some basic thermodynamic quantities (such as entropy and specific heat) that might exhibit a rather spectacular thermal dependences especially near the zero-temperature phase transitions. Furthermore, several interesting extensions and generalizations of the present version of the Ising-Heisenberg model come into question besides the most obvious ones mentioned at the end of Sec. II. For instance, it is possible to extend the present Ising-Heisenberg model by including higher-order triplet, quintuplet, and sextuplet interactions between the Ising and Heisenberg spins, or to solve exactly the analogous Ising-Heisenberg model with the Heisenberg spins $S > 1/2$ that accounts for other interaction terms such as the single-ion anisotropy and the biquadratic interaction. In this direction will continue our next work.

ACKNOWLEDGMENTS

This work was supported by the Slovak Research and Development Agency under Contract No. LPP-0107-06. The financial support provided by the Ministry of Education of Slovak Republic under Grant No. VEGA 1/0128/08 is also gratefully acknowledged.

[1] R. J. Baxter, *Exactly Solved Models in Statistical Mechanics* (Academic, New York, 1982).
[2] H. T. Diep and H. Giacomini, in *Frustrated Spin Systems*, edited by H. T. Diep (World Scientific, Singapore, 2004).
[3] D. A. Lavis and G. M. Bell, *Statistical Mechanics of Lattice Systems* (Springer, Berlin, 1999), Vol. 1.
[4] D. C. Mattis, *The Many-Body Problem: An Encyclopedia of Exactly Solved Models in One Dimension* (World Scientific, Singapore, 1993).
[5] E. H. Lieb, in *Condensed Matter Physics and Exactly Soluble Models*, edited by B. Nachtergaele, J. P. Solovej, and J. Yngvason (Springer, Berlin, 2004).
[6] B. Sutherland, *Beautiful Models: 70 Years of Exactly Solved Quantum Many-Body Problems* (World Scientific, Singapore, 2004).
[7] The term "Ising-Heisenberg model" might be a little bit confusing as it closely resembles the term "Heisenberg-Ising model," which is often used to refer to the *XXZ* Heisenberg models with the Ising-type anisotropy. Unlike this case, the term "Ising-Heisenberg model" will be strictly used in connection with hybrid models that consist of both Ising and Heisenberg spins.
[8] J. Strečka and M. Jaščur, Phys. Rev. B **66**, 174415 (2002).
[9] J. Strečka and M. Jaščur, Phys. Status Solidi B **233**, R12 (2002).
[10] J. Strečka and M. Jaščur, J. Magn. Magn. Mater. **272-276**, 987 (2004).
[11] M. Jaščur and J. Strečka, Czech. J. Phys. **54**, D587 (2004).
[12] J. Strečka and M. Jaščur, Acta Phys. Slov. **56**, 65 (2006).
[13] L. Čanová, J. Strečka, and M. Jaščur, J. Magn. Magn. Mater. **316**, e352 (2007).
[14] J. Strečka, L. Čanová, M. Jaščur, and M. Hagiwara, Phys. Rev. B **78**, 024427 (2008).
[15] D. X. Yao, Y. L. Loh, E. W. Carlson, and M. Ma, Phys. Rev. B **78**, 024428 (2008).
[16] L. Čanová, J. Strečka, J. Dely, and M. Jaščur, Acta Phys. Pol. A **113**, 449 (2008).
[17] M. Jaščur, J. Strečka, and L. Čanová, Acta Phys. Pol. A **113**, 453 (2008).
[18] I. Syozi, Prog. Theor. Phys. **6**, 306 (1951).
[19] L. Onsager, Phys. Rev. **65**, 117 (1944).
[20] M. E. Fisher, Phys. Rev. **113**, 969 (1959).
[21] I. Syozi, in *Phase Transitions and Critical Phenomena*, edited by C. Domb and M. S. Green (Academic, New York, 1972), Vol. 1, pp. 270–329.
[22] T. Utiyama, Prog. Theor. Phys. **6**, 907 (1951).
[23] C. Domb, Adv. Phys. **9**, 149 (1960).
[24] K. Y. Lin and S. F. Lee, Chin. J. Phys. (Taipei) **24**, 280 (1986).
[25] O. Rojas, J. S. Valverde, and S. M. de Souza, Physica A **388**, 1419 (2009).
[26] F. Y. Wu, Phys. Rev. B **4**, 2312 (1971).
[27] L. P. Kadanoff and R. J. Wegner, Phys. Rev. B **4**, 3989 (1971).
[28] R. J. Baxter, Phys. Rev. Lett. **26**, 832 (1971).
[29] R. J. Baxter, Ann. Phys. (N.Y.) **70**, 193 (1972).
[30] C. Fan and F. Y. Wu, Phys. Rev. **179**, 560 (1969).
[31] C. Fan and F. Y. Wu, Phys. Rev. B **2**, 723 (1970).
[32] M. Roger and J. M. Delrieu, Phys. Rev. B **39**, 2299 (1989).
[33] S. Sugai, M. Sato, T. Kobayashi, J. Akimitsu, T. Ito, H. Takagi, S. Uchida, S. Hosoya, T. Kajitani, and T. Fukuda, Phys. Rev. B **42**, 1045 (1990).
[34] Y. Honda, Y. Kuramoto, and T. Watanabe, Phys. Rev. B **47**, 11329 (1993).
[35] Y. Mizuno, T. Tohyama, and S. Maekawa, J. Low Temp. Phys. **117**, 389 (1999).
[36] R. Coldea, S. M. Hayden, G. Aeppli, T. G. Perring, C. D. Frost, T. E. Mason, S.-W. Cheong, and Z. Fisk, Phys. Rev. Lett. **86**, 5377 (2001).
[37] A. A. Katanin and A. P. Kampf, Phys. Rev. B **66**, 100403(R) (2002).
[38] M. Matsuda, K. Katsumata, R. S. Eccleston, S. Brehmer, and H.-J. Mikeska, Phys. Rev. B **62**, 8903 (2000).
[39] S. Notbohm, P. Ribeiro, B. Lake, D. A. Tennant, K. P. Schmidt, G. S. Uhrig, C. Hess, R. Klingeler, G. Behr, B. Büchner, M. Reehuis, R. I. Bewley, C. D. Frost, P. Manuel, and R. S. Eccleston, Phys. Rev. Lett. **98**, 027403 (2007).
[40] E. H. Lieb, Phys. Rev. Lett. **18**, 692 (1967).
[41] E. H. Lieb, Phys. Rev. **162**, 162 (1967).
[42] F. Y. Wu, Phys. Rev. Lett. **18**, 605 (1967).
[43] B. Sutherland, Phys. Rev. Lett. **19**, 103 (1967).
[44] E. H. Lieb, Phys. Rev. Lett. **19**, 108 (1967).
[45] E. H. Lieb, Phys. Rev. Lett. **18**, 1046 (1967).
[46] R. J. Baxter, Phys. Rev. Lett. **26**, 834 (1971).

[47] R. J. Baxter, Ann. Phys. (N.Y.) **76**, 1 (1973).
[48] R. J. Baxter, Ann. Phys. (N.Y.) **76**, 25 (1973).
[49] R. J. Baxter, Ann. Phys. (N.Y.) **76**, 48 (1973).
[50] R. J. Baxter, J. Stat. Phys. **108**, 1 (2002).
[51] G. E. Andrews, R. J. Baxter, and P. J. Forrester, J. Stat. Phys. **35**, 193 (1984).
[52] V. V. Bazhanov and V. V. Mangazeev, Nucl. Phys. B **775**, 225 (2007).
[53] V. Korepin and P. Zinn-Justin, J. Phys. A **33**, 7053 (2000).
[54] P. Zinn-Justin, Phys. Rev. E **62**, 3411 (2000).
[55] H. Cohn, R. Kenyon, and J. Propp, J. Am. Math. Soc. **14**, 297 (2001).
[56] K. Minami, J. Math. Phys. **49**, 033514 (2008).
[57] R. J. Baxter, J. Math. Phys. **11**, 784 (1970).
[58] R. J. Baxter, J. Math. Phys. **11**, 3116 (1970).
[59] E. H. Lieb and F. Y. Wu, in *Phase Transitions and Critical Phenomena* (Ref. [21]), Vol. 1, pp. 332–487.
[60] M. Suzuki, Prog. Theor. Phys. **51**, 1992 (1974).
[61] J. M. J. van Leeuwen, Phys. Rev. Lett. **34**, 1056 (1975).
[62] M. P. Nightingale, Phys. Lett. **59A**, 486 (1977).
[63] S. Krinsky and D. Mukamel, Phys. Rev. B **16**, 2313 (1977).
[64] R. H. Swendsen and S. Krinsky, Phys. Rev. Lett. **43**, 177 (1979).
[65] K. Binder and D. P. Landau, Phys. Rev. B **21**, 1941 (1980).
[66] J. Oitmaa, J. Phys. A **14**, 1159 (1981).
[67] K. Minami and M. Suzuki, Phys. Lett. A **180**, 179 (1993).
[68] K. Minami and M. Suzuki, Physica A **192**, 152 (1993).
[69] K. Minami and M. Suzuki, Physica A **195**, 457 (1993).
[70] K. Minami and M. Suzuki, J. Phys. A **27**, 7301 (1994).
[71] V. Vaks, A. Larkin, and Y. Ovchinnikov, Sov. Phys. JETP **22**, 820 (1966).
[72] T. Chikyu and M. Suzuki, Prog. Theor. Phys. **78**, 1242 (1987).
[73] P. Azaria, H. T. Diep, and H. Giacomini, Phys. Rev. Lett. **59**, 1629 (1987).
[74] P. Azaria, H. T. Diep, and H. Giacomini, Phys. Rev. B **39**, 740 (1989).
[75] H. T. Diep, M. Debauche, and H. Giacomini, Phys. Rev. B **43**, 8759 (1991).
[76] M. Debauche, H. T. Diep, P. Azaria, and H. Giacomini, Phys. Rev. B **44**, 2369 (1991).
[77] J. Stephenson, J. Math. Phys. **11**, 420 (1970).
[78] J. Stephenson, Can. J. Phys. **98**, 2118 (1970).
[79] J. Stephenson, Phys. Rev. B **1**, 4405 (1970).
[80] J. S. Valverde, O. Rojas, and S. M. de Souza, Phys. Rev. E **79**, 041101 (2009).